1983;1(2):541–9

DIAGNOSTIC TECHNIQUES

Differentiation of Constrictive Pericarditis and Restrictive Cardiomyopathy Using Digitized Echocardiography

GREGORY G. JANOS, MD,* KALAVATHY ARJUNAN, BA, RICHARD A. MEYER, MD, FACC, PETER ENGEL, MD, FACC, SAMUEL KAPLAN, MD, FACC

Cincinnati, Ohio

Constrictive pericarditis and restrictive cardiomyopathy are difficult to distinguish at the bedside and occasionally at routine cardiac catheterization. Left ventricular diastolic function was studied by computer analysis of digitized M-mode echocardiograms in four patients with constrictive disease and three with restrictive disease, and the data were compared with those of normal subjects. The respective distinguishing echographic features of constrictive pericarditis and restrictive cardiomyopathy were as follows: the major filling period of the left ventricle was 78 ± 9% of normal versus 128 ± 4% ($p < 0.01$), minimal left ventricular dimension to peak filling interval was 50 ± 10 versus 110 ms ($p < 0.05$) and the maximal rate of left ventricular posterior wall thinning was −4.9 versus −2.3 seconds^{-1} ($p < 0.05$). This preliminary study suggests that it may be possible to accurately diagnose the two disease entities using this technique at the bedside and to avoid cardiac catheterization.

Constrictive pericarditis and restrictive cardiomyopathy may be difficult to distinguish clinically and by cardiac catheterization. Differentiation of the two conditions by standard M-mode echocardiography has depended primarily on the identification of thickened pericardial echoes (1,2) and normal left ventricular ejection phase indexes in constrictive pericarditis compared with normal pericardial echoes and abnormal ejection indexes in restrictive cardiomyopathy (3–6). However, these findings are not consistently present in all patients.

Computer-assisted analysis of digitized M-mode echocardiograms has been used to study instantaneous rates of change in left ventricular chamber, septal and posterior wall dimensions (7–17). Digitizing the M-mode echocardiogram has proved helpful in defining disturbances of left ventricular diastolic function in those patients with ischemic cardiomyopathy (8), secondary ventricular hypertrophy (9,14,15), decreased left ventricular inflow (10,11,17), aortic insufficiency (12) and primary myocardial disease (15,16).

The primary pathophysiology in both of these conditions is an abnormality in ventricular filling. Because digitized echocardiography has been helpful in defining abnormalities of left ventricular filling, we believed it might also be used to better understand and perhaps to distinguish these clinically similar conditions. Hence, we studied left ventricular diastolic function by computer analysis of digitized M-mode echocardiograms in four patients with constrictive pericarditis and three patients with restrictive cardiomyopathy and compared them with normal echocardiograms.

Methods

Subjects

The study groups consisted of seven patients: Group I, three patients with restrictive cardiomyopathy and Group II, four patients with constrictive pericarditis (Table 1). Diagnosis was confirmed by autopsy in one patient (Case 1) and by surgery in five patients (Cases 3 to 7). The remaining patient (Case 2) had a history compatible with a hypereosinophilic cardiomyopathy. The M-mode echocardiograms from each patient in the study groups were digitized and analyzed prior to confirmation of their diagnosis.

Thirty-nine normal subjects, 20 female and 19 male, who had normal physical findings, electrocardiogram, chest radiogram and echocardiogram were studied. They ranged in age from 6 days to 16 years, mean 56 months, with age distribution as follows: 7, 0 to 3 months; 5, 4 months to 1 year; 13, 1 to 5 years and 14, over 6 years.

From the Division of Cardiology, Children's Hospital Medical Center and Division of Cardiology, Internal Medicine, University of Cincinnati College of Medicine, Cincinnati, Ohio. This study was supported in part by Grant HL-07417-02 from the U.S. Public Health Service, Bethesda, Maryland and American Heart Association, Southwestern Ohio Chapter, Cincinnati, Ohio. Manuscript received August 23, 1982, accepted September 23, 1982.

*Present address: Division of Pediatric Cardiology, University of California, Davis, Medical Center, Sacramento, California

Address for reprints: Richard A. Meyer, MD, Division of Cardiology, Children's Hospital Medical Center, Elland and Bethesda Avenues, Cincinnati, Ohio 45229.

0735-1097/83/020541-9$03 00

Table 1. Clinical Summary and M-Mode Echocardiographic Results in Patients With Restrictive Cardiomyopathy and Constrictive Pericarditis

Case	Age (yr)	Disease	Surgical Findings	Pathologic Findings	M-Mode Echogram: Thickened Pericardium	M-Mode Echogram: LVID	M-Mode Echogram: SF%	M-Mode Echogram: LVPEP/LVET
Restrictive Cardiomyopathy								
1	6	Id	NA	Myocardial fibrosis	0	3.6	22	0.53
2	14	Eo	NA	NA	0	3.8	21	0.55
3	21	Rad	Normal pericardium	NA	0	5.0	34	0 33
Constrictive Pericarditis								
4	40	TB	Thickened pericardium	NA	+	4 8	25	NA
5	9	Surg	Thickened pericardium	NA	0	2 4	46	0.33
6	67	TB	Thickened pericardium	NA	0	3.6	38	NA
7	37	Surg	Thickened pericardium	NA	+	3.3	42	NA

Eo = hypereosinophilic cardiomyopathy, Id = idiopathic myocardial fibrosis, LVET = left ventricular ejection time, LVID = left ventricular internal dimension, diastole, LVPEP = left ventricular pre-ejection period; NA = not accessible, Rad = radiation cardiomyopathy, SF% = percent shortening of left ventricular internal dimension, diastole; Surg = post-surgical pericarditis; TB = tuberculous, + = present, 0 = absent.

Digitized Echocardiography

Echocardiography. Standard M-mode echocardiograms were obtained with either a Picker 80C or Hoffrel unit using 2.25 to 5.0 MHz transducers with 6 to 13 mm active diameters and were interfaced to a Honeywell 1856 or Irex multichannel recorder. Simultaneous electrocardiograms and respirations obtained by impedance plethysmography were recorded with the echograms at paper speeds of 50, 75 or 100 mm/s. Recordings of the left ventricular endocardium were made just inferior to the mitral valve sulcus as previously described (18). Left ventricular systolic time intervals were obtained in the standard fashion at a paper speed of 100 mm/s (18). Only those records with a well defined left ventricular posterior wall and normal interventricular septal motion were digitized using a Digisonic Echo-Comp M-mode calculator and image analyzer consisting of a sonic digitizer, an on-line minicomputer and a printer. Changes in left ventricular cavity dimension and posterior wall during systole and diastole were analyzed.

Measurement and calculations. The digitizer resolution M was 0.25 mm (0.01 inch). The uncertainty in time interval measurement (in ms) was calculated from the formula: $\Delta T = \Delta M \sqrt{\frac{2}{p}}$, where ΔT = the uncertainty in time, ΔM = the digitizer resolution and P = paper speed. Thus, for paper speeds of 50, 75 and 100 mm/s the ΔT was 7.0, 4.6 and 3.5 ms, respectively. The uncertainty in distance measurement (in mm) is expressed as: $\Delta D = \Delta M \sqrt{\frac{2}{S}}$, where ΔS = the uncertainty in distance and S = depth scale (mm/cm calibration mark). For depth scales that measured 5, 10 and 20 mm/cm of tissue, the ΔD was 0.7, 0.4 and 0.2 mm, respectively. To minimize these errors, the echocardiograms obtained prospectively were recorded at paper speeds of 100 mm/s and the depth scale was expanded 1.5 to 2 times the actual size.

The error in calculation of rates of change of dimension is dependent on the depth scale, paper speed, ΔM and the sampling rate. For this system, the sampling rate was every 5 ms for dimension with resampling every 20 ms for rate of change of dimension. The application of a five-point smoothing filter to the calculated dimension reduced the maximal error of rates of dimension change to no greater than 12% when using rapid paper speed and expanded depth scale.

Calibration of the digitizer was accomplished by touching the digitizer pen to the time markers of the M-mode echogram 1 second apart and to the depth markers at 3 cm apart. The heart rate was derived from the RR interval of the electrocardiogram. Two consecutive cardiac cycles at end-expiration (each cycle included two successive Q waves) were digitized with the measurements taken from the first of the two cycles in all instances. Whenever possible, cardiac cycles at different heart rates from the same patient were recorded and analyzed for differences.

Continuous traces of the leading edge of the endocardium of the posterior wall and the posterior edge of the left septal surface represented the left ventricular chamber (Fig. 1). Likewise, traces of the posterior wall thickness were made by tracing the leading edge of the endocardium and the epicardial-pericardial interface. Traces of the septal thickness were not done because of the frequent difficulty in identifying the leading edge of the right septal surface. The string of data points was analyzed by the minicomputer every 5 ms and printed in tabular form every 10 ms. Chamber dimension and wall thickness with their rates of change were plotted every 20 ms (Fig. 2).

The rate of change (in seconds^{-1}) of chamber dimensions was normalized by the instantaneous dimension $(\frac{dD}{dt} \cdot \frac{1}{D})$ (Fig. 2),

J AM COLL CARDIOL
1983;1(2):541-9

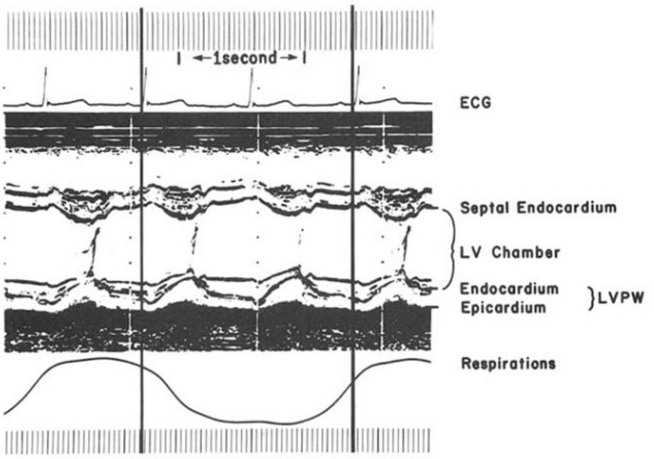

Figure 1. Normal echogram of left ventricle (LV) from which computer analysis of digitized chamber and left ventricular posterior wall (LVPW) can be made. ECG = electrocardiogram.

whereas the rate of change in thickening and thinning $(\frac{dTn}{dt} \cdot \frac{1}{Tn})$ of the wall was normalized by maximal thickness (Fig. 3). The latter two variables were normalized for maximal dimensions because we found that compared with the relatively smaller posterior wall dimension (normal range 0.2 to 1.0 cm), small pen movements resulted in large swings in the instantaneous rate of change.

Measurements were then made easily and directly from the plots of reading on the appropriate axis corresponding to the points of interest. For example, in Figure 2, the normalized peak rate of left ventricular filling (max $\frac{dD}{dt} \cdot \frac{1}{D}$ diastole) and the Q–peak rate of filling interval are 4.0 seconds^{-1} and 0.5 second, respectively. All of the values reported were obtained by this technique.

In order to minimize intra- and interobserver errors of measurement, the boundaries of the echoes of the left septal surface, left posterior endocardium and epicardium were agreed on and then outlined with a lead pencil before tracing with the sonic pen. To test for interobserver differences, 17 cycles from four normal subjects were digitized by the first observer. A second observer independently digitized the same cycles. Intraobserver error was tested by digitizing a single cardiac cycle consecutively 10 times by the same person. This was done on cycles recorded from the same patient at identical heart rates but at a paper speed of 50 mm/s, at a depth scale of 13 mm/cm and with unpenciled tracings and finally at a paper speed of 100 cm/s, at a depth scale expanded to 20 mm/cm and with penciled outlines.

Definition of Terms

Left ventricular chamber (Fig. 2). 1. Q–minimal dimension = the interval from the onset of the QRS complex to the point of minimal chamber dimension, where $\frac{dD}{dt} \cdot \frac{1}{D} = 0$ and corresponds to end-systole.

2. Max $\frac{dD}{dt} \cdot \frac{1}{D}$ diastole = the maximal rate of increase of the chamber dimension during diastole and corresponds to the peak rate of filling. The interval from the onset of the QRS complex to

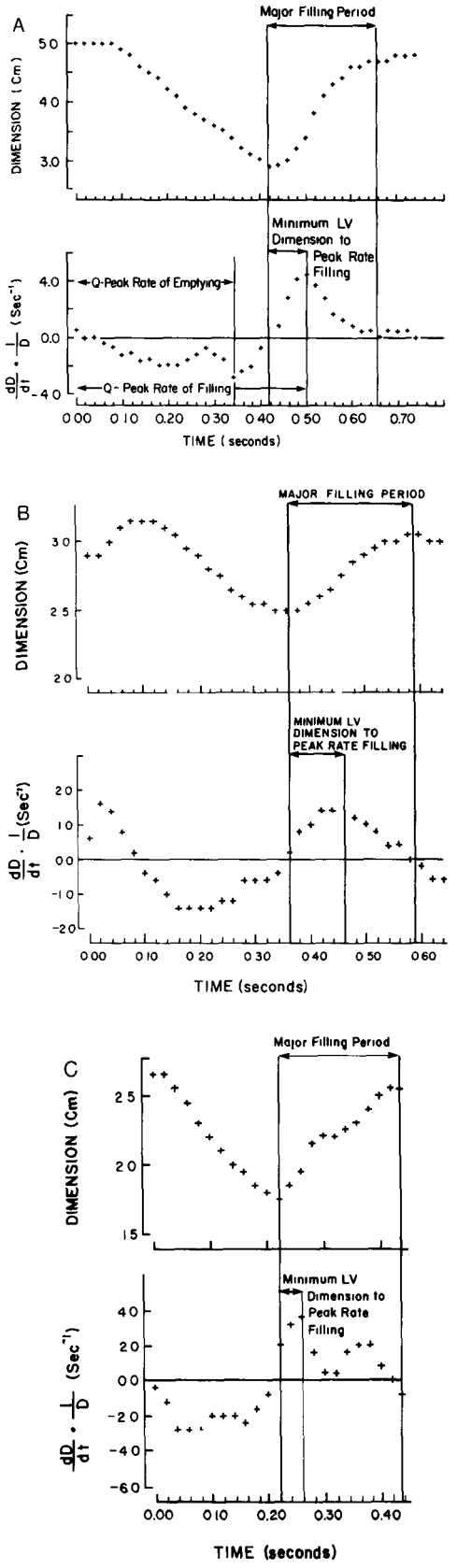

Figure 2. Digitized plot of the computer analysis from a single cycle of a normal (**A**), restrictive (**B**) and constrictive (**C**) left ventricular (LV) chamber. The rate of change $\left(\frac{dD}{dt}\right)$ of the chamber dimension as well as the dimensional change are shown.

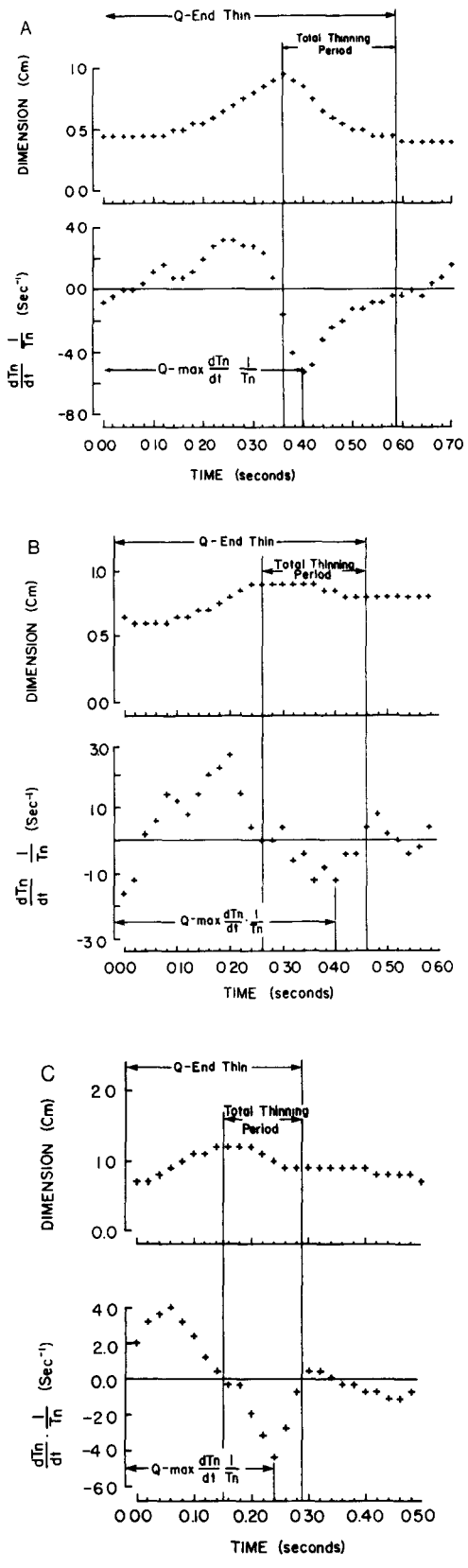

Figure 3. Digitized plot of the computer analysis from a single cycle of a normal (**A**), restrictive (**B**) and constrictive (**C**) left ventricular posterior wall. The rate of thinning $\frac{dTn}{dt}$ as well as the change in dimension and the indexes measured are shown

the point of maximal rate of increase in dimension is the Q–peak rate of filling.

3. Minimal chamber dimension to peak rate of filling = the interval from the minimal dimension to the peak rate of filling.

4. Major filling period = the interval from the point of minimal chamber dimension to the point on the curve where $\frac{dD}{dt} \cdot \frac{1}{D}$ first returns to zero. This interval also includes the isovolumic relaxation period. We did not include simultaneous phonocardiograms in our study and were therefore unable to measure the isovolumic relaxation period interval from the aortic component of the second heart sound to the onset of mitral valve opening (14). In addition, timing of the opening of the mitral valve by echocardiography remains controversial (15–17). We found that in subjects with a rapid heart rate, it is particularly difficult to consistently determine the onset of valve opening from their echograms. Thus, the major filling period includes the isovolumic relaxation period, the rapid filling phase, slow filling phase and most of atrial systole and is expressed as a percent of normal.

Left ventricular posterior wall (Fig. 3). 1. Max $\frac{dTn}{dt} \cdot \frac{1}{Tn}$ = the maximal rate of diastolic thinning.

2. Q–max $\frac{dTn}{dt} \cdot \frac{1}{Tn}$ = the interval from the onset of the QRS complex to the point of maximal rate of diastolic thinning.

3. Q–end of thinning = the interval from the onset of the QRS complex to the end of diastolic thinning where the $\frac{dTn}{dt} \cdot \frac{1}{Tn}$ first equals zero and the wall plateaus on the dimension curve.

4. Total thinning period = the interval from the point of maximal systolic thickness to the end of thinning.

Standard M-mode echocardiography. In addition to the digitized variables, standard chamber dimensions and percent shortening fraction of the left ventricular and pericardial thickness were determined from the M-mode echograms of each subject (Table 1).

Statistical analysis. Student's *t* test for unpaired samples was used to test significant difference of the mean of the digitized variable between the normal and study groups. Because the heart rate in children varies considerably according to age, we evaluated the effect of heart rate on all the indexes using regression analysis. Correlation was performed by linear regression and calculation of the Pearson's correlation coefficient.

Results

Digitized Analysis

Observer error. The interobserver differences are expressed as the root mean square differences for the paired results. The root mean square differences for $\frac{dD}{dt} \cdot \frac{1}{D}$ diastole and $\frac{dTn}{dt} \cdot \frac{1}{Tn}$ posterior wall were 0.4 and 0.5 second^{-1}, respectively. The intraobserver errors from the cycle measured at the faster paper speed with the expanded depth

Table 2. Summary of Intraobserver Error (mean ± SD)

Index	Cycle A	Cycle B
$\frac{dD}{dt} \cdot \frac{1}{D}$ Systole	$-3.8 \pm 1.1\ s^{-1}$ (-2.7 to -5.7)	$-2.8 \pm 0.35\ s^{-1}$ (-2.4 to -3.4)
$\frac{dD}{dt} \cdot \frac{1}{D}$ Diastole	$3.9 \pm 1.0\ s^{-1}$ (2.9 to 6.0)	$3.6 \pm 0.65\ s^{-1}$ (2.6 to 4.7)
$\frac{dTk}{dt} \cdot \frac{1}{Tk}$ LVPW	$5.4 \pm 1.5\ s^{-1}$ (3.4 to 8.1)	$3.3 \pm 0.59\ s^{-1}$ (2.5 to 4.3)
$\frac{dTn}{dt} \cdot \frac{1}{Tn}$ LVPW	$-7.2 \pm 1.7\ s^{-1}$ (-4.5 to -10.2)	$-6.2 \pm 1.5\ s^{-1}$ (-3.7 to -8.2)

Figures in parentheses indicate range of values
Cycle A = paper speed 50 mm/s, depth scale 13 mm/cm and unpenciled, cycle B = paper speed 100 mm/s, depth scale 20 mm/cm and penciled; LVPW = left ventricular posterior wall, SD = standard deviation. See text for explanation of indexes

scale and penciled outline were substantially less than those obtained from the slower compressed and unpenciled tracing (Table 2).

Normal subjects. From the echograms of the 29 normal subjects, 81 individual cardiac cycles were analyzed. The rhythm in all was sinus and the heart rate ranged from 55 to 195 beats/min (mean ± standard deviation 110 ± 32). The Q–minimal dimension (Q to end-systole) was obtained from 100% of the cardiac cycles. The success rate for the other indexes ranged from 67 to 94%: major filling period (89%), total thinning period (67%) and Q–end thinning of the wall (72%). Problems in determining these indexes were related to the occasional absence of a clear-cut "plateau" in the dimension curve corresponding to the end of the interval (Fig. 2). Difficulties in determining the intervals from the Q wave to the peak rate of change of dimensions for both the chamber and wall (78 to 94%) were the result of having multiple peaks in the rate of change curves (Fig. 3). This occurred most commonly in the echograms taken at slower speeds and smaller depth scales where the error in measurement was greatest. Indeed, this problem was virtually eliminated when the measurements were made from the echograms obtained with the paper speed at 100 mm/s and the depth scale at 10 to 20 mm/cm.

The time intervals and rates of change of dimension for both chamber and wall thickness were related to heart rate by single regression analysis ($r > 0.50$, $p < 0.05$) (Table 3). Neither the peak rate of filling ($\max \frac{dD}{dt} \cdot \frac{1}{D} = 3.2 \pm 0.8$ second^{-1}, mean ± standard deviation) nor the peak thinning rate of the posterior wall ($\max \frac{dTn}{dt} \cdot \frac{1}{Tn} = 6.3 \pm 1.5$ second^{-1}) was strongly related to heart rate. All of the intervals with one exception were strongly and inversely related to heart rate. The exception was the minimal chamber dimension to peak rate filling interval (0.08 ± 0.02 second), which tended to be shorter at faster heart rates ($r = 0.30$) but exhibited considerable scatter of data. The major filling period ($r = -0.79$), Q–peak rate of filling ($r = -0.83$), Q–maximal rate thinning ($r = -0.76$) and Q–end thinning ($r = -0.80$) were all strongly correlated to heart rate ($p < 0.01$ in each); the total thinning period was slightly less ($r = -0.64$, $p < 0.01$).

Patients with restrictive and constrictive disease. Because the rates of change of chamber and posterior wall dimension and the minimal chamber dimension to peak rate of filling interval were not heart rate-dependent, they were averaged for each group. The other intervals were corrected for heart rate using the regression equations (Table 3), expressed as percent of normal, and averaged for each group.

Chambers. The mean maximal filling rate was significantly lower in patients with restrictive cardiomyopathy (2.3 seconds^{-1}) than in patients with constrictive pericarditis (3.1 seconds^{-1}) or normal subjects, although there was overlap in data (Fig. 4). However, the major filling period was significantly prolonged in restrictive cardiomyopathy (128

Table 3. Regression Equations Relating Computer Analysis Indexes to Heart Rate in Normal Subjects

Equation	n	SEE	r Value	p
Systolic				
Q–end thickening (LVPW) × 100 = −0.15 HR + 50	62	±7	−0.68	<0.01
Q–minimum LV dimension × 100 = −0.17 HR + 50	81	±6	−0.85	<0.01
Q–peak rate of emptying (LV) × 100 = −0.10 HR + 25	75	±5	−0.58	<0.01
Diastolic				
Major filling period (LV) × 100 = −0.12 HR + 35	72	±5	−0.79	<0.01
Q–peak rate of filling (LV) × 100 = −0.19 HR + 59	76	±8	−0.83	<0.01
Q–max $\frac{dTn}{dt} \cdot \frac{1}{Tn}$ (LVPW) × 100 = −0.20 HR + 60	63	±8	−0.76	<0.01
Q–end thinning (LVPW) × 100 = −0.29 HR + 77	58	±10	−0.80	<0.01
Total thinning period (LVPW) × 100 = −0.11 HR + 26	54	±5	−0.65	<0.01

HR = heart rate; LV = left ventricular; LVPW = left ventricular posterior wall; n = number of determinations, p = probability, r = correlation coefficient, SEE = standard error of the estimate

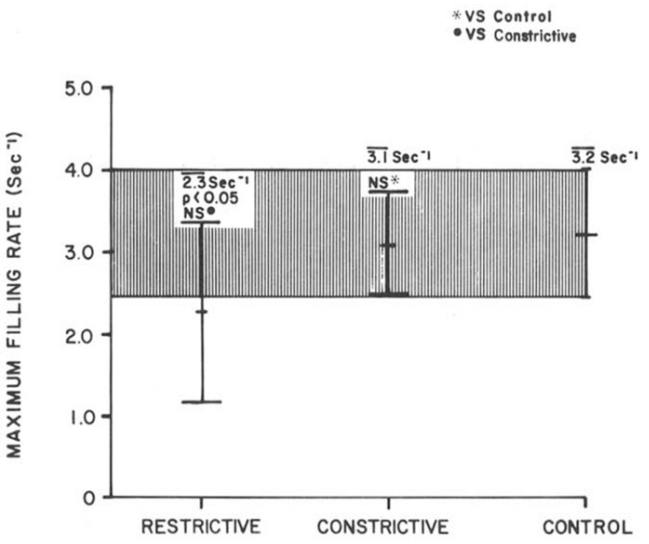

Figure 4. Comparison of maximal filling rate (mean ± standard deviation) of the left ventricular chamber in patients with restrictive and constrictive disease and in normal control-subjects (**hatched area** and **horizontal bars**). * = probability (p) value versus (VS) control subjects. • = p value versus patients with constrictive disease; NS = not significant.

± 4% of normal) and abbreviated in constrictive pericarditis (78 ± 9% of normal) with no overlap in data (Fig. 5). The minimal dimension to peak rate of filling interval was significantly prolonged in restrictive cardiomyopathy (110 ± 30 ms) but shortened in constrictive pericarditis (50 ± 10 ms) with a wide separation of data (Fig. 6).

Posterior wall. The maximal thinning rate in restrictive cardiomyopathy was subnormal (-2.3 seconds^{-1}) and markedly slower than in constrictive pericarditis (-4.9 seconds^{-1}) which was not significantly different from normal (Fig. 7); there was no overlap of data between constrictive and restrictive disease. The total thinning period of the wall was prolonged in both study groups (144 ± 32% and 126 ± 17%) with considerable overlap of data (Fig. 8).

To summarize, the variables that best allowed differentiation of patients with restrictive from those with constrictive disease were the major filling period, minimal dimension to peak filling interval and maximal thinning rate of the wall.

Figure 5. Comparison of major filling period of left ventricle in patients with restrictive and constrictive disease and in normal control subjects expressed as a percent of normal ± standard deviation (SD). Format as in Figure 4

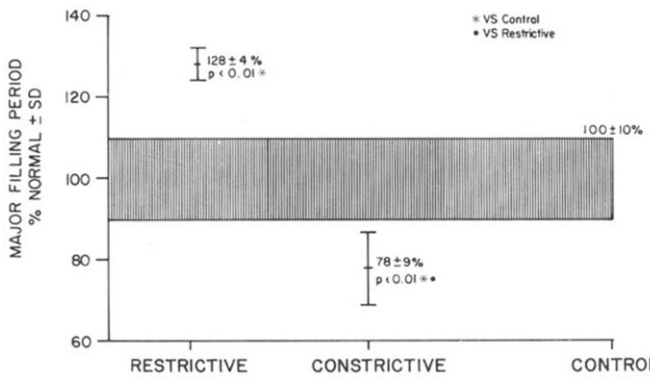

M-Mode Data (Table 1)

None of the patients with restrictive cardiomyopathy but two of the four patients with proved constrictive pericarditis had thickened pericardial echoes. The left ventricular internal dimension at end-diastole was large in only one patient (Case 1) who had restrictive disease and was normal in the remaining patients. Indexes of systolic function were abnormal in Patients 1 and 2 with restrictive disease, who had a low shortening fraction (normal 28 to 42%) and a prolonged left ventricular systolic time interval ratio (normal 0.28 to 0.04). Patient 6 with constrictive pericarditis had a shortening fraction of 25%. None of these differences in the standard echographic variables between the two groups were significant and could differentiate the two conditions.

Discussion

Methodologic considerations. One goal of this study was to provide a standard reproducible approach to the computer analysis of digitized M-mode echocardiograms. Many errors in measurements of digitized M-mode tracings are a function of basic digitizer resolution and image size. Most commercial systems include smoothing filters to reduce tracing jitter and our system uses a five-point smoothing filter. Operator artifact occurs primarily from hand motion while tracing the echogram with the digitizer pen. Some of this artifact can be eliminated through practice. However, to further improve the quality of our digitized plots and reduce the errors of measurement, we adopted three additional techniques: 1) record the echogram at rapid paper speed (100

Figure 6. Comparison of the interval between left ventricular (LV) minimal dimension to peak filling from patients with restrictive and constrictive disease and normal control subjects. Format as in Figure 4.

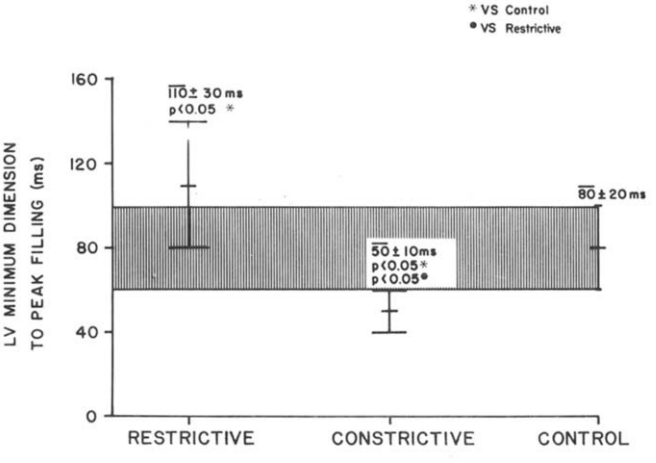

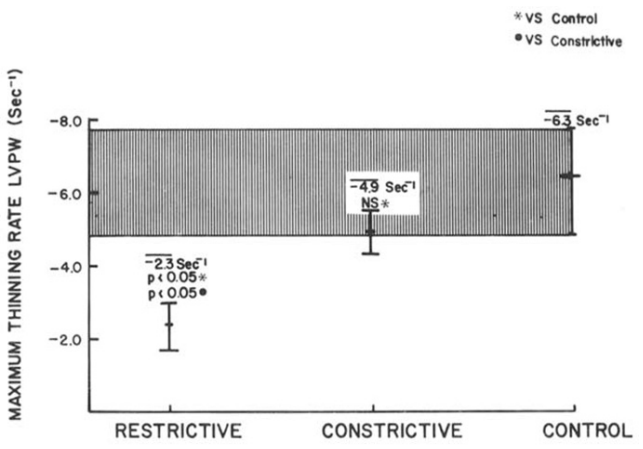

Figure 7. Comparison of maximal thinning rate of the left ventricular posterior wall (LVPW) from patients with restrictive and constrictive disease and normal control subjects. Format as in Figure 4.

mm/s), 2) use expanded depth scale (>10 mm/cm), and 3) determine which echo interface shall be used and trace it with a lead pencil before digitizing. Although other investigators have stressed the importance of obtaining the M-mode records at rapid paper speed (7–11) little emphasis has been placed on the effect of depth scale or system error. Because the errors in time interval measurement ($\triangle T$) and distance measurement ($\triangle D$) in our system are inversely proportional to paper speed and depth scale, respectively, doubling these variables reduced our intraobserver error by half (Table 3). In addition, by determining which echo will be used before digitizing and tracing the echoes with pencil, we produced smoother, more reproducible plots at the various paper speeds tested and reduced the interobserver error. Even though we tested the sum and not the individual effect these three variables had on the measurement error, we considered that each was important to improve reproducibility and accuracy.

Normal digitized values. The rates of change for the wall and chambers of the left ventricle in our normal subjects were unaffected by heart rate, which is in agreement with other investigations that included children and adults (7,8,13–16,19). Our values for maximal thinning rate (-6.3 ± 1.5) were normalized for maximal dimension and therefore were different from the only other reported value (-8.69 ± 4.33 second^{-1}) of St. John Sutton et al. (11), who normalized for instantaneous dimension. The minimal dimension to peak rate of filling interval was the only interval not significantly related to heart rate. This interval mainly consists of the isovolumic relaxation period, which has been shown to be very weakly correlated to heart rate (20–23), but it was relatively short and small changes secondary to heart rate effect were difficult to discern. The major filling period and total thinning period are both relatively longer intervals and constitute the majority of diastole. The fact that they are significantly affected by heart rate is expected because the duration of both systole and diastole is determined by the cycle length. The timing of peak filling of the ventricle and that of thinning of the wall are both strongly affected by heart rate, and these events occur simultaneously as reflected in the near identity of the regression equation relating them to heart rate. Because left ventricular filling is thought to occur as the result of relaxation or thinning of the myocardium, the peak rate of filling would be expected to occur simultaneously with the time of maximal wall relaxation or thinning. Traill et al. (24) also found that the peak rate of thinning coincided with the peak rate of increase in chamber dimension during diastole.

Figure 8. Comparison of total thinning period of the left ventricular posterior wall (LVPW) from patients with restrictive and constrictive disease and normal control subjects expressed as percent. Format as in Figure 4.

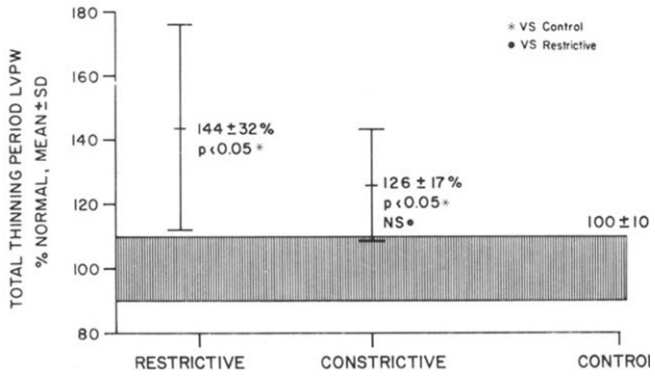

Chamber filling and relaxation in constrictive pericarditis versus restrictive cardiomyopathy. The M-mode echocardiographic findings in each group of our patients with constrictive pericarditis and restrictive cardiomyopathy were individually consistent with previously published reports (2–4,25–28); however, routine M-mode echocardiography has not been previously used to distinguish the two. With the variability of the echographic findings in both diseases, it was not possible in our few patients to separate these two disease entities by routine M-mode analysis. The lack of specific echographic features may result from subtle differences in the various disease states that result in restriction of filling or differences in severity and duration of the diseases. By utilizing computer analysis of digitized M-mode echograms we demonstrated abnormalities of chamber filling and wall relaxation that were widely disparate in patients with constrictive pericarditis and restrictive cardiomyopathy and that allowed differentiation of the two conditions.

The increased maximal filling rate and shortened major filling period found in constrictive pericarditis plus the reduced maximal filling rate and prolonged major filling period found in restrictive cardiomyopathy are consistent with the work of Tyberg et al. (29). From pressure-volume loops obtained by cardiac catheterization and cineangiography, they showed significant differences in the pattern of filling in normal subjects and in patients with constrictive peri-

carditis and restrictive cardiomyopathy. The diastolic filling curve in normal subjects had a rapid slope in early diastole, which corresponded to the "rapid filling phase," followed by a gradual smooth slope for the remainder of diastole. At 50% of diastole, 65% of ventricular filling had occurred. The curves from patients with constrictive pericarditis had a very rapid filling slope during the first half of diastole with a plateau throughout the remainder of diastole; that is, by 50% of diastole, 85% of ventricular filling had occurred. In restrictive cardiomyopathy, the curves demonstrated a rapid filling phase that was indistinguishable from normal but was uniformly slower and had a prolonged mid-diastolic filling phase; that is, at 50% of diastole, only 45% of ventricular filling had occurred. Thus the data from both of our studies suggest that ventricular filling occurs more completely and earlier in patients with constrictive pericarditis than in those with restrictive cardiomyopathy. We were able to discern absolute differences in the timing and magnitude of the peak filling rate of the left ventricular chamber in the two groups because we plotted the instantaneous rate of change in dimension versus time.

The mechanisms causing differences in filling patterns in the two conditions are unknown. The most plausible explanation is that in constrictive pericarditis the hindrance to ventricular filling does not occur until the chamber reaches a size limited by the nondistensible pericardium; however, in restrictive cardiomyopathy hindrance to filling occurs throughout diastole from the poorly compliant and diseased myocardium. The digitized echographic index of poor wall thinning was highlighted in our patients with restrictive cardiomyopathy, suggesting that in these patients the disorder in ventricular filling was the result of a primary disease process affecting myocardial relaxation. Development of experimental models for constrictive pericarditis and restrictive cardiomyopathy with further investigation by digitized echographic and pressure-loop analysis may be necessary to resolve this problem. Studies of this type might also establish a relation between the severity of the condition and the digitized echographic findings so that quantitation will be possible.

Implications. Although our patient numbers were small, the findings in each group of patients were consistent and significant differences in the digitized M-mode echogram were observed in patients with constrictive pericarditis and restrictive cardiomyopathy. In fact, there was wide separation of several indexes in the two groups. We hope that further studies involving more patients will verify our findings and validate the accuracy and reliability of digitized echocardiography. As our understanding of the pathophysiologic differences of these clinically similar conditions improves, selection of patients who may require exploratory thoracotomy should likewise improve and it should be possible to obviate cardiac catheterization.

Addendum

We have seen an additional adult patient with constrictive pericarditis who underwent exploratory surgery to establish the diagnosis after completion of this study. Without knowledge of the surgical results, we were able to make the correct preoperative diagnosis from the digitized echographic findings.

We extend our sincere appreciation to Cathy Hoover for preparation of the manuscript and to Diana McSherry, PhD, for her technical assistance.

References

1. Feigenbaum H. Echocardiography, 3rd ed. Philadelphia: Lea & Febiger, 1981:496–502.
2. Schnittger I, Bowden R, Abrams J, Popp R. Echocardiography: pericardial thickening and constrictive pericarditis. Am J Cardiol 1978; 42:388–95.
3. Khullar S, Lewis R. Usefulness of systolic time interyals in differential diagnosis of constrictive pericarditis and restrictive cardiomyopathy. Br Heart J 1976;38:43–6.
4. Ghose JC, Mitra SK, Chhetri MK. Systolic time intervals in the differential diagnosis of constrictive pericarditis and cardiomyopathy. Br Heart J 1976;38:47–50.
5. Armstrong TG, Lewis BS, Gotsman MS. Systolic time intervals in constrictive pericarditis and severe primary myocardial disease. Am Heart J 1973;85:6–12.
6. Lewis BS, Gotsman MS. Left ventricular function in systole and diastole in constrictive pericarditis. Am Heart J 1973;86:23–41.
7. Gibson DG, Brown DJ. Measurement of instantaneous left ventricular dimension and filling rate in man using echocardiography. Br Heart J 1973;35:1141–9.
8. Upton MT, Gibson DG, Brown DJ. Echocardiographic assessment of abnormal left ventricular relaxation in man. Br Heart J 1976;38:1001–9.
9. Gibson DG, Traill TA, Hall RJC, Brown DJ. Echocardiographic features of secondary left ventricular hypertrophy. Br Heart J 1979;41:54–9
10. St John Sutton MG, Traill TA, Ghafour AS, Brown DJ, Gibson DG. Echocardiographic assessment of left ventricular filling after mitral valve surgery. Br Heart J 1977,39:1283–91.
11. St John Sutton MG, Tajik AJ, Gibson DG, Brown DJ, Seward JB, Giuliani EF. Echocardiographic assessment of left ventricular filling and septal and posterior wall dynamics in idiopathic hypertrophic subaortic stenosis. Circulation 1978;57:512–20.
12. Venco A, St John Sutton MG, Gibson DG, Brown DJ. Noninvasive assessment of left ventricular function after correction of severe aortic regurgitation. Br Heart J 1976;38:1324–31.
13. St John Sutton MG, Hagler DJ, Tajik AJ, et al. Cardiac function in the normal newborn: additional information by computer analysis of the M-mode echocardiogram. Circulation 1978;57:1198–204.
14. Friedman M, Sahn D, Birris H, Allen H, Goldberg S. Computerized echocardiographic analysis to detect abnormal systolic and diastolic left ventricular function in children with aortic stenosis. Am J Cardiol 1979;44:478–86.
15. Kugler JD, Gutgesell HP, Nihill MR. Instantaneous rates of left ventricular wall motion in infants and children. Pediatr Cardiol 1979;1:15–21.
16. Goldberg SJ, Feldman L, Reinecke C, Stern L, Sahn DJ, Allen HD. Echocardiographic determination of contraction and relaxation measurements of left ventricular wall in normal subjects and patients with muscular dystrophy. Circulation 1980;62:1061–9

17. St John Sutton MG, Meyer RA, Tajik AJ, Ritman EL. Computer analysis of the echocardiogram in newborns with persistent fetal circulation (abstr). Am J Cardiol 1979;43:385.

18. Meyer RA. Pediatric Echocardiography. Philadelphia: Lea & Febiger, 1977:70–83.

19. Hammermeister KD, Warbasse JR. The rate of change of left ventricular volume in man. II. Diastolic events in health and disease. Circulation 1974;49:739–47.

20. Harrison TR, Dixon K, Russell RO Jr, Bidwai PS, Coleman HN. The relation of age to the duration of contraction, ejection and relaxation of the normal human heart. Am Heart J 1964;67:189–99.

21. Arevalo F, Sakamoto T. On the duration of the isovolumetric relaxation period (IVRP) in dogs and man. Am Heart J 1965;67:651–6.

22. Benchimol A. Ellis JG. A study of the period of isovolumic relaxation in normal subjects and in patients with heart disease. Am J Cardiol 1967;19:196–206.

23. Spitaels S, Arbogast R, Fouron JC, et al. The influence of heart rate and age on the systolic and diastolic time intervals in children. Circulation 1974;49:1107–15.

24. Traill TA, Gibson DG, Brown DJ. Study of left ventricular wall thickness and dimension changes using echocardiography. Br Heart J 1978;40:162–9.

25. Voelkel AG, Pietro DA, Folland ED, Fisher ML, Parisi AF. Echocardiographic features of constrictive pericarditis. Circulation 1978;58:871–5.

26. Candell-Riera J, Castillo G, Permanyer-Miralda G, Soler-Soler J. Echocardiographic features of the interventricular septum in chronic constrictive pericarditis. Circulation 1978;57:1154–8.

27. Borer JS, Henry WL, Epstein SE. Echocardiographic observations in patients with systemic infiltrative disease involving the heart. Am J Cardiol 1977;39:184–8.

28. Benotti JR, Grossman W, Cohn PF. Clinical profile of restrictive cardiomyopathy. Circulation 1980;61:1206–12.

29. Tyberg TI, Goodyer AVN, Hurst VW, Alexander J, Langou RA. Left ventricular filling in differentiating restrictive amyloid cardiomyopathy and constrictive pericarditis. Am J Cardiol 1981;47:791–6.